Measuring the adhesion of alumina coatings onto Fecralloy supports using a mechanical testing system

Adegbite, Stephen

DOI:
10.1016/j.apsusc.2012.07.046

Document Version
Publisher's PDF, also known as Version of record

Citation for published version (Harvard):
Adegbite, S 2012, 'Measuring the adhesion of alumina coatings onto Fecralloy supports using a mechanical testing system', *Applied Surface Science*, vol. 259, pp. 338-342. https://doi.org/10.1016/j.apsusc.2012.07.046

Applied Surface Science 259 (2012) 338–342

Contents lists available at SciVerse ScienceDirect

Applied Surface Science

journal homepage: www.elsevier.com/locate/apsusc

Measuring the adhesion of alumina coatings onto Fecralloy supports using a mechanical testing system

S.A. Adegbite*

Engineering and Physical Sciences, University of Birmingham, Birmingham B15 2TT, UK

ARTICLE INFO

Article history:
Received 12 March 2012
Received in revised form 26 June 2012
Accepted 9 July 2012
Available online 16 July 2012

Keywords:
Fecralloy
Adhesion
Coating
Alumina
Support
Mechanical
Catalyst

ABSTRACT

Tightening legislation for vehicles across the world has caused the use of monolith catalysts in automotive emission control to become ubiquitous. Control of the surface adhesion of the platinum group metal (PGM) coating onto the monolith block, to maximise catalytic performance for a minimum PGM loading, is therefore paramount. In this paper, an automatic film application is used for coating γ-alumina slurries onto Fecralloy®, an integral component of metallic monolith catalysts, to achieve the desired coating properties. A newly devised dual compression–tension technique using a mechanical testing system (MTS) is used for measuring the coating adhesion. This method involves compression of the coating with a probe at a fixed load, and then removing the probe together with the coating at right angles to the substrate surface at a speed of 10 mm/min. The MTS results are compared with those from conventional ultrasonic vibration tests. It is found that at 40 wt% solids concentration, the coatings of the finest particles ($d_{0.9}$ of 12.14 μm) showed the best adhesion with an ultimate strength of 0.59 MPa and 85–90 mass% coating removal.

1. Introduction

From 1940 to 1950s air quality problems were experienced in some urban cities in the USA because of the increasing numbers of cars [1,2]. The first major applications of monolith catalysts during this period were for automotive emission control and for the decolourisation of nitric acid tail gas. In the late 1960s researchers in the USA began to develop more interests in monoliths in their quest for effective afterburner catalysts because of their characteristic low pressure drop. This led to the development and industrial production of monolith catalysts of increased longevity which would meet the requirements of the 1970 Clean Air Act [3,4]. The emergence of the first cars equipped with monolith catalysts began in 1975. Today there are several hundred millions of monolith catalysts fitted in motor vehicles worldwide [5].

Throughout the last three decades the advancements in emission control technology have been propelled by stringent legislation. One major success worth noting is that since 1975 emission levels from exhaust systems of passenger cars have fallen by more than 90% (relative to the 1960s), with future targets aimed at zero emissions [6]. The exhaust gas stream consists of 3 major pollutants: carbon monoxide (CO), oxides of nitrogen (NO) and hydrocarbons (HCs). This stream is converted inside the exhaust pipe, which houses the catalyst, into environmentally less harmful products (such as nitrogen gas and carbon dioxide). Monolith catalysts are manufactured in industry by coating γ-alumina slurries – the carrier of the platinum group metals (PGMs) – onto structured catalyst supports. These catalysts are essentially used in environmental applications but also in chemical and construction processes [7]. Monoliths are honeycomb materials (Fig. 1) that act as catalyst supports (or substrates) upon which coating slurries are deposited. They are of two types: metallic monoliths, made from Fecralloy®; and ceramic monoliths, mostly made from cordierite [8]. Metal monoliths have significantly thinner walls compared to ceramic monoliths, and this enables the former to have a much shortened warm-up period which leads to increased catalytic efficiency [9,10]. On the other hand, ceramic monoliths are relatively cheap and have large pores which absorb the slurry, and this improves the coating adhesion. The thermal expansion of the coating is also similar to ceramic monoliths compared to metal [7]. These problems can however be tackled by proper slurry formulation, and the use of metal monoliths which are based on an appropriate alloy, such as Fecralloy®, that is specially processed to form an adherent and stable alumina surface layer [11,12].

Literature survey has shown that the main method of coating Fecralloy® in the laboratory is by dip-coating [9,12–14], though other methods have been used, such as electrophoretic deposition [10], and physical vapour deposition which can be cathodic sputtering, electron-beam evaporation or pulsed laser deposition [15]. Each of these coating methods has its advantages and

* Corresponding author. Tel.: +44 0 1483 689312.
E-mail address: s.adegbite@surrey.ac.uk

0169-4332/$ – see front matter © 2012 Elsevier B.V. All rights reserved.
http://dx.doi.org/10.1016/j.apsusc.2012.07.046

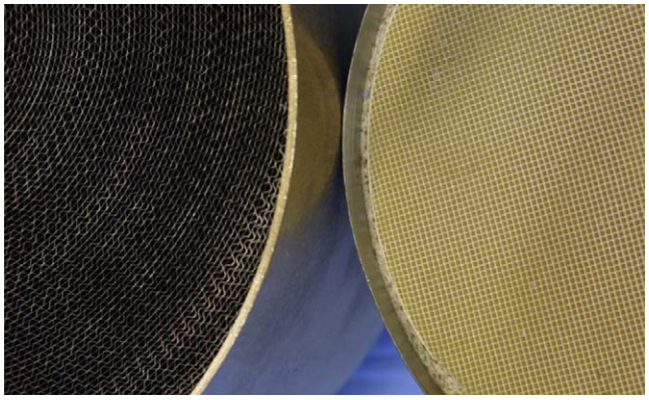

Fig. 1. Examples of metal-based catalyst (left) and ceramic-based cordierite catalyst (right).

disadvantages, and the method to be chosen in a given application depends on the required coating properties [16]. The common disadvantage of dip-coating is the inconsistency in the coating quality as evidenced from the wide variation in the coating loadings [12]. There is therefore a need to develop a more consistent laboratory-scale method of coating Fecralloy® to produce the desired coating properties. In this paper, an automatic film applicator equipped with wire-wound bars is chosen as the coating instrument because it had been designed to enable control of the coating conditions, such as applied shear rate [17].

The adhesion of coatings onto the Fecralloy® is fundamental to the longevity and effectiveness of the monolith catalyst. As there are mechanical and thermal stresses inside the exhaust system of automobiles, the coating adhesion needs to be sufficient to resist these stresses [18]. There is urgent need to devise new methods for measuring the coating adhesion because none of the conventional methods (e.g. ultrasonic vibration, drop test) give a physical measure of the adhesive or cohesive strength of coatings. A physically derived method is established when the measured coating variables are based on fundamental scientific quantities, such as tensile stress, displacement and compression load [19]. This paper focuses on how slurry particle sizes influence the coating adhesion and the advantages of using the MTS for assessing coatings. This approach involves measuring the adhesion of alumina coatings onto Fecralloy® flat coupons, and is therefore different from measuring the adhesion of already constructed monoliths, which are comprised of channels with an additional component of the adhesion due to constriction produced by the high curvature of the coatings inside the small channels [18,20]. The MTS technique is the main method for assessing coatings in this paper, while ultrasonic vibration is used as a subordinate. The empirical characterisation of slurries (i.e. particle size analyses and rheology) is also performed prior to coating of slurries onto the Fecralloy® coupons by the film applicator.

2. Experimental

2.1. Preparation of slurries and coatings

2.1.1. Preparation of slurries

The γ-alumina slurries S_{S10}–S_{S240} (pH 4; solids concentration = 40 wt%) were prepared in a stirred bead mill (Union Process, USA) at different milling durations between 10 and 240 min. The particle size distributions and the steady shear rheology of the slurries were measured using the Mastersizer 2000 (Malvern Instruments, UK) and the AR 1000 rheometer (TA Instruments, UK) respectively.

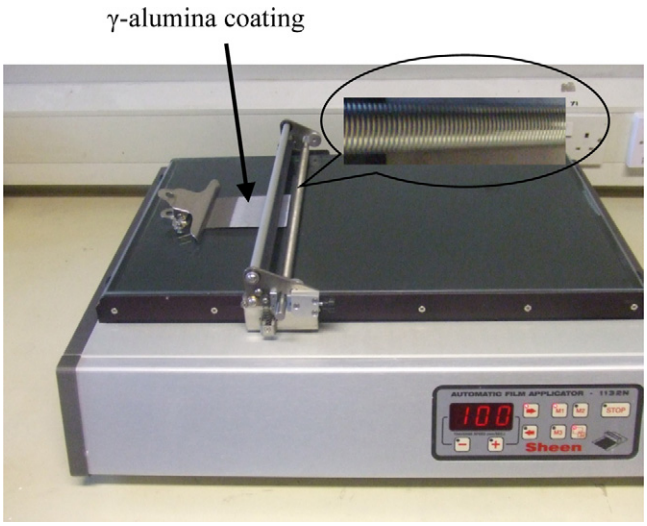

Fig. 2. A automatic film applicator showing how coating was done.

2.1.2. Fecralloy® pre-oxidation

Commercially available Fecralloy® foil of 50 μm thickness with a composition of Fe (72.6 wt%), Cr (22.0 wt%), Al (4.80 wt%), Y (0.30 wt%) and Si (0.30 wt%) was cut into coupons (50 × 80 mm) and pre-oxidised in a furnace at 950 °C for 10 h.

2.1.3. Coating deposition

The automatic film applicator was used to coat the slurries described in (a) separately onto the coupons using a bar of 100 μm nominal gap at a traverse speed of 100 mm s^{-1} (shear rate = 1000 s^{-1}) as shown in Fig. 2. The coated coupons were allowed to dry at room temperature, and then oven dried at 110 °C for 1 h and finally calcined at 500 °C for 1 h [12,21].

2.2. MTS methodology for assessing coating adhesion

The MTS is comprised of a dual column which houses a load cell of 1 kN. Each coating sample produced in Section 2.1.3 was firmly screwed onto the platform base of the MTS using an annular support (Fig. 3(a)). A metal probe was mounted at one end to the MTS, and the other end was joined with a carbon tape and lowered to make contact with the coating. The programming of the probe was such that the coating was compressed at a specified load (Fig. 3(b)). The probe was then lifted up at a given withdrawal speed of 10 mm/min, which consequently resulted in the detachment of the coating from the Fecralloy® substrate. The coating remaining on the substrate is shown in Fig. 3(c), and the probe with the detached coating is shown in Fig. 3(d). The measurements taken were converted into graphs of stress versus displacement using the test profiler software which linked the MTS to a computer.

A typical profile obtained from the MTS is represented in Fig. 4. This shows a drop in the applied compression stress as the probe was being lifted up. The point of zero is the equilibrium, i.e. the instance when no force was acting on the probe. The stress increased thereafter as the probe continued to move up, thus representing the start of tension. The moment of complete rupture (or removal) of the coating is referred to as the breaking point and the corresponding stress at this point is called the ultimate strength [22]. The stress dropped to zero after the breaking point as the probe was finally released from tension. The ultimate strength is a very important parameter for quantifying the adhesion strength of the coating. The amount of coating removed, which is dependent on the contact area of the probe, was the mass% difference in the coatings on the substrate before and after the test.

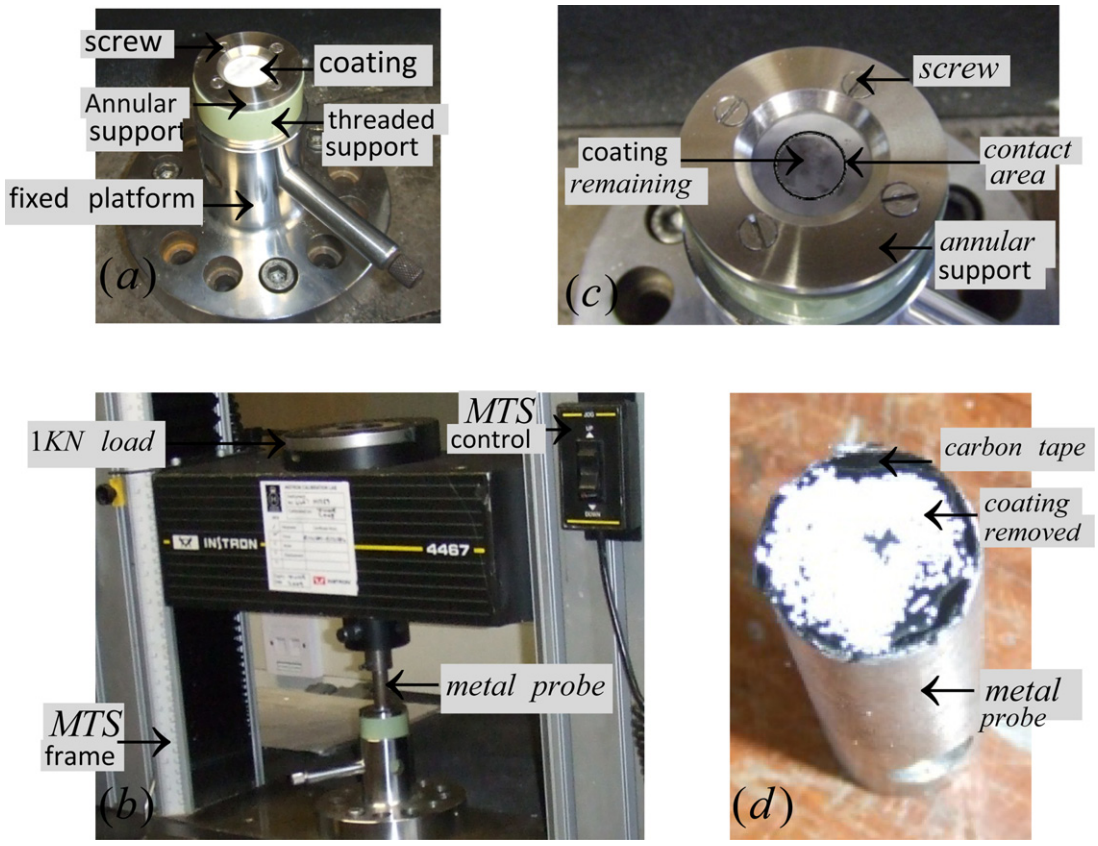

Fig. 3. Pictures showing how coating adhesion is being measured by MTS: (a) coating firmly screwed; (b) coating compressed by probe; (c) coating remaining after test and (d) probe showing coating removed.

The portion of the graph above the zero line (i.e. shaded area) is referred to as the work of adhesion, which is defined as the energy per unit area required to remove the coating from the substrate as shown in Eq. (1) [23]. This was calculated by Simpson's rule using Matlab® (The MathWorks, USA).

$$w_{adh} = \int_{h_{crit}}^{h_{break}} S_p dh = \int_{h_{crit}}^{h_{break}} \frac{F_p}{A} dh = \frac{1}{A} \int_{h_{crit}}^{h_{break}} F_p dh \quad (1)$$

where w_{adh} = work of adhesion (kJ m^{-2}), s_p = stress on coating due to tension (MPa), F_p = force on coating due to tension (kN), h_{crit} = displacement at stabilisation stress (mm), h_{break} = displacement at breaking point (mm), A = contact area (mm^2).

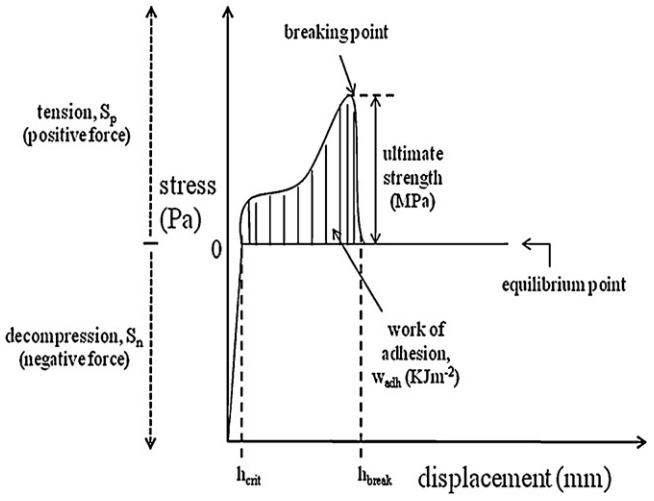

Fig. 4. MTS profile showing fundamental parameters measured.

Preliminary MTS tests were performed on coatings from slurry S_{S60} at different compression loads of 100, 200 and 300 N to determine the effects of compression on the coating adhesion. Subsequently, the adhesion for all the coatings were measured at a fixed compression load of 200 N using the methodology described. For comparison, the coating adhesion was also assessed by ultrasonic vibration.

3. Results and discussion

3.1. Particle size distribution and rheology

The particle size distributions of the slurries are outlined in Table 1, as well as the slurry apparent viscosity at a reference shear rate of 1000 s^{-1} at which the coating was applied. The results show a systematic decrease in the particle diameters with the increase in milling time, from 10 to 240 min as large particles were fragmented into finer particles. Furthermore, the increase in the effective phase volume of the particles as they become finer (and closely packed together) contributed to an increase in the slurry viscosity [24,25].

3.2. Influence of compression load on coating adhesion

For coatings produced from slurries S_{S60}, the MTS profiles at different compression loads of 100, 200 and 300 N are shown in Fig. 5. The plots show a drop in the stress at A due to the decompression occurring as the probe was being pulled upwards. An equilibrium point of zero was reached and thereafter the stress began to increase at tension, thus leading to an offset at B. The offset, which

Table 1
Slurry particle diameters and rheology at solids concentration of 40 wt%.

Slurry type	Bead milling time (min)	$d_{0.1}$ (μm)	$d_{0.5}$ (μm)	$d_{0.9}$ (μm)	Viscosity at reference shear rate of 1000 s^{-1} (mPa s)
S_{S10}	10	2.64	15.16	33.42	12.2
S_{S20}	20	1.90	9.56	23.02	12.8
S_{S40}	40	1.71	6.13	16.47	12.9
S_{S60}	60	1.34	4.36	12.74	13.7
S_{S240}	240	1.09	2.76	7.82	15.0

10 vol% of particles have diameters less than $d_{0.1}$
50 vol% of particles have diameters less than $d_{0.5}$
90 vol% of particles have diameters less than $d_{0.9}$

Table 2
MTS results for coatings from slurry S_{S60} at different compression loads.

Compression force (N)	Offset B (MPa)	Ultimate strength C (MPa)	Amount removed (mass% contact area)	Work of adhesion (kJ m^{-2})
100	0.29	0.59	86–90	0.34
200	0.27	0.59	85–90	0.33
300	0.32	0.59	85–89	0.33

varies between 0.27 and 0.32 MPa, is analogous to the coating yield strength and is considered as the stress required for disruption of the cohesive forces in the coatings at the onset of detachment [26]. The stress levelled slightly thereafter, followed by a notable increase in the stress until the ultimate strength was attained at C. This region represents the breaking point when the coatings were detached from the substrate. It is shown that the same ultimate strength of 0.59 MPa was achieved for all the compression loads. Following coating detachment, the stress reached equilibrium at D due to the upward free movement of the probe. The MTS results are summarised in Table 2. The ultimate strength for the removal of coatings was the same for all the compression loads, meaning therefore that the ultimate strength was independent on the compression load between 100 and 300 N. The work of adhesion and the amount of coatings removed were calculated as between 0.33–0.34 kJ m^{-2} and 85–90 mass% respectively.

3.3. Influence of particle size on coating adhesion

The coatings used in these tests were produced from slurries S_{S10}, S_{S40} and S_{S60}. Fig. 6 shows the MTS profiles of the stress as a function of displacement for all the coatings assessed. All the three plots have similar profiles: decompression until the stress was zero at equilibrium, followed by increased stress at tension until the ultimate strength was attained at coating removal, and finally the attainment of equilibrium. It is shown that the ultimate strength – which is the determinant of the adhesion quality – is dependent on the particle diameter of coatings. The highest ultimate stress of 0.59 MPa, inferring best adhesion, was achieved by the coatings from slurry S_{S60} ($d_{0.9}$ of 12.74 μm), followed by 0.29 MPa for S_{S40} ($d_{0.9}$ of 16.47 μm), and then the least ultimate strength of 0.10 MPa from S_{S10} ($d_{0.9}$ of 33.42 μm). Similarly, the ultimate strength and the work of adhesion both followed the same trend as they all increased with finer coating particles. Furthermore, the coating amounts removed were influenced by the particle diameter $d_{0.9}$ as presented in the detailed results shown in Table 3.

In addition to requiring the lowest ultimate strength of 0.10 MPa, the coatings from large particles were almost totally removed (more than 97 mass%) from the contact surface area. The finest coatings, on the other hand, had the least removal (85–90 mass%) at the highest ultimate strength of 0.59 MPa (see coating pictures in Fig. 7). These behaviours confirm cohesive failure (i.e. internal coating fractures) for fine particles rather than adhesive failure (i.e. coating peeling off the surface) exhibited by large particles.

The measurements by ultrasonic vibration given in Table 4 also show the same pattern, i.e. low mass% coating loss by finer particles. For finer particles of $d_{0.9}$ not exceeding 12.74 μm, the coating loss from ultrasonic vibration was less than 10 mass% coating loss.

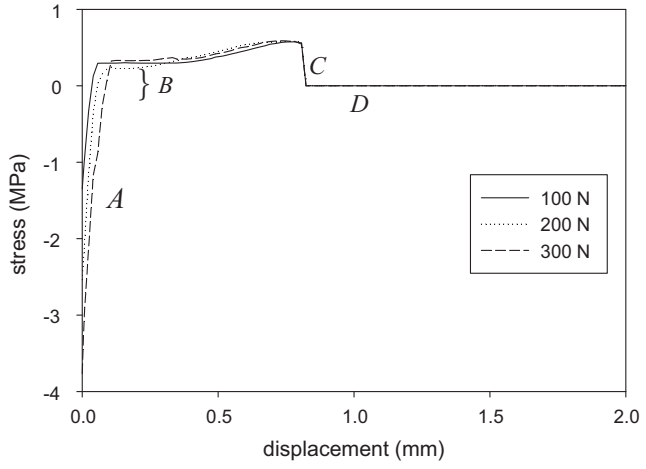

Fig. 5. Tensile stress versus displacement at different compression loads.

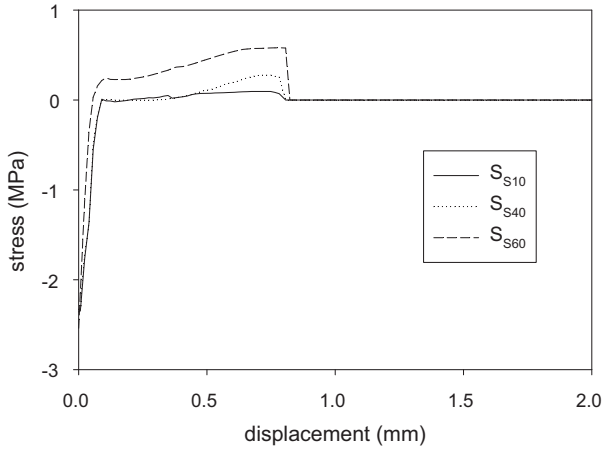

Fig. 6. MTS profiles for coatings from slurries S_{S10}, S_{S40} and S_{S60}.

Table 3
MTS results for coatings from slurries S_{S10}, S_{S40} and S_{S60}.

Slurry type	Diameter $d_{0.9}$ (μm)	Ultimate strength (MPa)	Amount removed (mass% contact area)	Work of adhesion (kJ m^{-2})
S_{S10}	33.42	0.10	>97	0.03
S_{S40}	16.47	0.29	88–93	0.07
S_{S60}	12.74	0.59	85–90	0.33

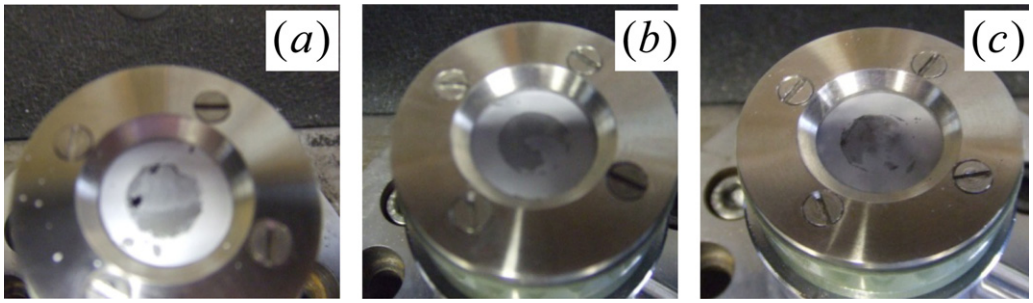

Fig. 7. Coating pictures after MTS tests showing amounts removed: (a) S_{S10};. (b) S_{S40} and (c) S_{S60}.

Table 4
Ultrasonic vibration results for coatings from slurries S_{S10}–S_{S240}.

Slurry type	$d_{0.9}$ (μm)	Coating loading (mass%) SD = ±2.5% of loading	Average film thickness (±2 μm)	Mass % loss from adhesion test SD = ±3.3% of loss
S_{S10}	33.42	7.4	53	37.3
S_{S20}	23.02	7.5	44	28.0
S_{S40}	16.47	8.1	40	15.5
S_{S60}	12.74	8.0	38	9.9
S_{S240}	7.82	7.8	37	8.0

This is because finer particles, unlike their large counterparts, properly penetrated and anchored onto the rough asperities on the Fecralloy® surface, therefore leading to good coating adhesion. It is therefore established from all the results that finer particles had better coating adhesion.

4. Conclusions

A new quantitative technique based on the MTS was used for measuring of adhesion of coatings of different particle sizes. The MTS technique involves the compression of the coating by a probe at a specified load, and subsequently lifting the probe upwards at a withdrawal speed of 10 mm/min, and as a result pulling off the coating. The force imposed on the coating by the probe was measured as a function of displacement. The adhesion parameters were identified as the ultimate coating strength, work of adhesion and the amount of coating removed from the substrate. It was shown that the use of compression loads from 100 to 300 N had no effect on the coating adhesion. For the coatings produced from the slurries at 40 wt% solids concentration, the finest particles ($d_{0.9}$ of 12.14 μm) produced the best coating adhesion at an ultimate strength of 0.59 MPa and 85–90 mass% removal. The finest particles also had the least mass percentage loss from ultrasonic vibration test. The coating pictures after the MTS test showed that finer coatings exhibited cohesive failure arising from internal coating fractures rather than the adhesive failure exhibited by large coatings.

Acknowledgments

The author would like to thank the Engineering and Physical Sciences Research Council (EPSRC) and Johnson Matthey Plc for funding this research project.

References

[1] A. Haagen-Smith, C.E. Bradley, M.M. Fox, Industrial & Engineering Chemistry 45 (1953) 2086.
[2] A. Haagen-Smith, M.M. Fox, Journal of Air Pollution Control Association 4 (1954) 136.
[3] A. Cybulski, J.A. Moulijn, Chemical Engineering Science 49 (1994) 19.
[4] A. Nievergeld, Automative Exhaust Gas Conversion: Reaction Kinetics, Reactor Modelling and Control, PhD, University of Technology, Eindhoven, 1998.
[5] M.V. Twigg, Applied Catalysis B: Environmental 70 (2007) 2.
[6] M.V. Twigg, Catalysis Today 117 (2006) 407.
[7] J.L. Williams, Catalysis Today 69 (2001) 3.
[8] P. Avila, M. Montes, E.E. Miro, Chemical Engineering Journal 109 (2005) 11.
[9] W. Fei, S.C. Kuiry, Y. Sohn, S. Seal, Surface Engineering 19 (2003) 189.
[10] H. Sun, X. Quan, S. Chen, H.M. Zhao, Y.Z. Zhao, Applied Surface Science 253 (2007) 3303.
[11] N. Burgos, M.A. Paulis, M. Montes, Journal of Materials Chemistry 13 (2003) 1458.
[12] L.W. Jia, M.Q. Shen, J. Wang, Surface and Coatings Technology 201 (2007) 7159.
[13] M. Valentini, G. Groppi, C. Cristiani, M. Levi, E. Tronconi, P. Forzatti, Catalysis Today 69 (2001) 307.
[14] S. Zhao, J.Z. Zhang, D. Weng, X.D. Wu, Surface and Coatings Technology 167 (2003) 97.
[15] H. Kestenbaum, A.L. de Oliveira, W. Schmidt, F. Schuth, W. Ehrfeld, K. Gebauer, H. Lowe, T. Richter, D. Lebiedz, I. Untiedt, H. Zuchner, Industrial and Engineering Chemistry Research 41 (2002) 710.
[16] V. Meille, Appl, Applied Catalysis A: General 315 (2006) 1.
[17] The automatic film applicator (manual), Sheen Instruments Ltd., UK, (2006).
[18] A. Cybulski, J.A. Moulijn, Structured Catalysis and Reactors, Taylor & Francis, London, 2006.
[19] C. Xu, S. Li, Proceedings of the ASME International Conference on Manufacturing Science and Engineering, 2007, p. 887.
[20] L.C. Almeida, F.J. Echave, O. Sanz, M.A. Centeno, J.A. Odriozola, M. Montes, Studies in Surface Science and Catalysis 175 (2010) 25.
[21] D. Truyen, M. Courty, P. Alphonse, F. Ansart, Thin Solid Films 495 (2006) 257.
[22] E.J. Pavlina, C.J. Van Tyne, Journal of Materials Engineering and Performance 17 (2008) 888.
[23] Y. Wei, J.W. Hutchinson, International Journal of Fracture 93 (1998) 315.
[24] H.A. Barnes, Journal of Non-Newtonian Fluid Mechanics 94 (2000) 213.
[25] R.L. Hoffman, Journal of Rheology 36 (1992) 947.
[26] M.F. Ashby, D.R.H. Jones, Engineering Materials 1, 2nd ed., Butterworth-Heinemann, Oxford, 1996, pp. 77.